A canonical EF-loop directs Ca^{2+}-sensitivity in phospholipase C-η2†

Petra Popovics[1], Jin Lu[2], L. Nadia Kamil[1], Kevin Morgan[3], Robert P. Millar[3,4], Ralf Schmid[5], Claudia A. Blindauer[2] and Alan J. Stewart[1]*

[1]School of Medicine, University of St Andrews, St Andrews, UK.

[2]Department of Chemistry, University of Warwick, Coventry, UK.

[3]MRC Human Reproductive Sciences Unit, Queen's Medical Research Institute, Edinburgh, UK.

[4]Mammal Research Institute, University of Pretoria, Pretoria, South Africa. [5]Department of Biochemistry, University of Leicester, Leicester, UK.

'Correspondence: Dr Alan J. Stewart, Medical and Biological Sciences Building, University of St Andrews, North Haugh, St Andrews, Fife, KY16 9TF, UK. Tel: +44 1334 463546; Fax: +44 1334 463482; E-mail: ajs21@st-andrews.ac.uk.

Abbreviations: $[Ca^{2+}]_i$, intracellular free Ca^{2+} concentration; CaM, calmodulin; DAG, 1,2-diacylglycerol; DMEM, Dulbecco's modified Eagle's medium; IP_3, inositol 1,4,5-trisphosphate; NCS-1, neuronal calcium sensor-1; NOESY, nuclear Overhauser effect spectroscopy; PH, pleckstrin homology; PIP_2, phosphatidylinositol 4,5-bisphosphate; PLC, phospholipase C; TOCSY, total correlation spectroscopy.

Abstract

Phospholipase C-η(PLCη) enzymes are a class of phosphatidylinositol 4,5-bisphosphate-hydrolyzing enzymes involved in intracellular signaling. PLCη2 can sense Ca^{2+} (stimulated by ~1 μM free Ca^{2+}) suggesting that it can amplify transient Ca^{2+} signals. PLCη enzymes possess an EF-hand domain composed of two EF-loops; a canonical 12-residue loop (EF-loop 1) and a non-canonical 13-residue loop (EF-loop 2). Ca^{2+}-binding to synthetic peptides corresponding to EF-loops 1 and 2 of PLCη2 and EF-loop 1 of calmodulin (as a control) was examined by 2D-[^{1}H,^{1}H] TOCSY NMR. Both PLCη2 EF-loop peptides bound Ca^{2+} in a similar manner to that of the canonical calmodulin EF-loop 1, particularly at their N-terminus. A molecular model of the PLCη2 EF-hand domain, constructed based upon the structure of calmodulin,

suggested both EF-loops may participate in Ca^{2+}-binding. To determine whether the EF-hand is responsible for Ca^{2+}-sensing, inositol phosphate accumulation was measured in COS7 cells transiently expressing wild-type or mutant PLCη2 proteins. Addition of 70μM monensin (a Na^{+}/H^{+} antiporter that increases intracellular Ca^{2+}) induced a 4 to 7-fold increase in wild-type PLCη2 activity. In permeabilized cells, PLCn2 exhibited a ~4-fold increase in activity in the presence of 1 μM free Ca^{2+}. The D256A (EF-loop1) mutant exhibited a ~10-fold reduction in Ca^{2+}-sensitivity and was not activated by monensin, highlighting the involvement of EF-loop 1 in Ca^{2+}-sensing. Involvement of EF-loop 2 was examined using D292A, H296A, Q297A and E304A mutants. Interestingly, the monensin responses and Ca^{2+}-sensitivities were largely unaffected by the mutations, indicating that the non-canonical EF-loop 2 is not involved in Ca^{2+}-sensing.

Key words: calcium; cell signaling; comparative modeling; EF-hand; phospholipase C; signal transduction.

Introduction

The intracellular movement of Ca^{2+} in response to the chemical messenger inositol 1,4,5-trisphosphate (IP_3) triggers a range of physiological processes. Upon activation, Ca^{2+} is released from intracellular stores into the cytoplasm whereby the intracellular free Ca^{2+} concentration ($[Ca^{2+}]_i$) rises from ~10^{-7} M to ~10^{-6} M (Berridge *et al.*, 2000). Generally, this increase in $[Ca^{2+}]_i$ results in the activation of effector proteins; where the binding of Ca^{2+} alters the proteins' conformation. This is then translated, often through a complex of proteins, into a physiological event. Many of these Ca^{2+}-effector proteins contain homologous Ca^{2+}-binding domains termed EF-hands (Strynadka and James, 1989; Gifford *et al.*, 2007).

Structurally, EF-hand domains consist of one or more pairs of EF-loops, each of which constitutes a structurally independent, functional domain (Drabikowski *et al.*, 1982). Each EF-loop (usually but not always) binds Ca^{2+} and links two α-helices positioned roughly perpendicular to one another forming a helix-loop-helix structure. Within the EF-hand these two motifs are stacked against one another in a face-to-face manner. This structure is further stabilized by a short antiparallel *β*-sheet formed between the pairs' EF-loops (Grabarek, 2006). The structural and metal ion-binding properties of these domains are reviewed by Gifford *et al.* (2007). Examples of Ca^{2+}-responsive effector proteins that contain EF-hand domains include calmodulin (CaM; Vetter and Leclerc, 2003), neuronal calcium sensor-1 (NCS-1; Burgoyne, 2004) and troponin C (Parmacek and Leiden, 1991). EF-hand (or EF-hand-like) domains are also present in the mammalian phosphatidylinositol 4,5-bisphosphate (PIP_2)-specific phospholipase C (PLC) enzymes. Once activated these enzymes catalyze the cleavage of PIP_2 to generate the secondary messengers 1,2-diacylglycerol (DAG) and IP_3. DAG activates protein kinase C whilst IP_3 triggers the release of Ca^{2+} from intracellular stores. The EF-hand domains of most of these enzymes have limited or no ability to bind

Ca^{2+} (Bairoch and Cox, 1990). A key exception to this is PLCζ, which is responsible for Ca^{2+} oscillations in fertilized oocytes and exhibits a high sensitivity to Ca^{2+} mediated through its EF-hand domain (Kouchi *et al.*, 2005). Also it appears that the EF-hand domain of PLCδ1 is functionally important and regulates binding of the pleckstrin homology (PH) domain to PIP_2 in a Ca^{2+}-dependent manner (Yamamoto *et al.*, 1999).

The most recent class of mammalian PLC enzyme to be identified - the PLCη enzymes, are most closely related to the PLCδ class (Stewart *et al.*, 2005; Nakahara *et al.*, 2005; Hwang *et al.*, 2005; Zhou *et al.*, 2005). Two putative PLCη enzymes are present in humans and mice, PLCη1 and PLCη2 (Stewart *et al.*, 2005). Both catalyze hydrolysis of PIP_2 (Nakahara *et al.*, 2005; Hwang *et al.*, 2005; Zhou *et al.*, 2005), which suggests that these enzymes, like other PIP_2-specific PLCs, are involved in the production of DAG and IP_3. The cellular function of these enzymes is not entirely clear, although a recent study highlighted a potential role for PLCη2 in regulating neurite growth (Popovics *et al.*, 2013). It has become apparent that both PLCη enzymes are activated by intracellular Ca^{2+} mobilization (Kim *et al.*, 2011; Popovics *et al.*, 2011), and are sensitive to changes in $[Ca^{2+}]_i$ within the physiological range (Nakahara *et al.*, 2005; Hwang *et al.*, 2005). This discovery provides a rationale for the existence of a positive-feedback loop for Ca^{2+}, whereby PLCη enzymes can modulate further (or sustained) release of Ca^{2+} from intracellular stores through production of the secondary messenger, IP_3. In this study we demonstrate that the submicromolar Ca^{2+}-sensitivity of PLCη2 is directed by a functional EF-hand domain.

Materials and Methods

Materials

The peptides used in this study (CaM-EF1, Ac-LFDKDGDGTITTKEL; η2-EF1, Ac-EADKNGDGSLSIGE; η2-EF2, Ac-EADTDDHQGTLGFEE) were synthesized by EZBiolab (Westfield, IN, USA). The expression construct encoding residues 75-1238 of mouse PLCη2 (isoform a; NP_780765) in pcDNA3.1 (as used in Nakahara *et al.*, 2005) was a gift from Prof. Kiyoko Fukami (Tokyo University of Pharmacy and Life Science, Japan). This construct was used to synthesize D256A, D292A, H296A, Q297A and E304A mutants using the Quikchange Site-Directed Mutagenesis Kit (Stratagene, Amsterdam, The Netherlands).

NMR studies

1D and 2D [^{1}H,^{1}H] TOCSY (60 ms mixing time, using an MLEV-17 (Bax and Davis, 1985) sequence for spin-lock) and NOESY (500 ms mixing time) spectra were acquired at 298 K on 1 mM samples in DMSO-d_6, both in the presence and absence of 5 mM $CaCl_2$, on a Bruker DRX500 spectrometer, operating at 500.13 MHz for 1 h. Residual water was suppressed using excitation sculpting with gradients (Hwang and Shaka, 1995). All datasets were acquired with a spectral width of 13 ppm, using 4k data points in F2, 400 increments in F1, and the States-TPPI (time-proportional phase incrementation; Marion *et al.*, 1989) acquisition mode. Spectra were processed with TopSpin v. 2.1, using shifted sine-bell functions for apodization in both dimensions, and Fourier-transformed using 2k×2k data points. The residual DMSO peak at 2.51 ppm was used for calibrating all spectra. In all but one case (the NH resonance for K13 in calmodulin EF-loop 1 was not observed) complete sequential assignment was achieved using routine methods and the visualization and assignment program Sparky v. 3.111. The resulting chemical shifts for backbone protons were used to

explore the effects of Ca^{2+}. The dipolar aprotic solvent DMSO-d_6 was chosen because signals for labile protons such as those of the NH backbone protons, are often reduced or missing in aqueous media due to exchange with bulk water but readily observed in DMSO. Most peptides have good solubility in DMSO, and a large number of conformational studies of short peptides have been carried out in DMSO-d_6 (Oliva *et al.*, 2000), including studies on Ca-binding peptides (Gaggelli *et al.*, 1999). It is noteworthy that DMSO does not induce secondary structure (Yeagle *et al.*, 2007), can act as an H-bond acceptor, but not a donor, and has a weaker tendency than water to co-ordinate to metal ions. Based on the lower dielectric constant (46.7) and the slightly lower Gutmann donicity of DMSO (Marcus, 1984), the tendency for Ca^{2+}-peptide binding is expected to be moderately increased in DMSO, compared to aqueous solutions.

Inositol phosphate release assays

Plasmids encoding wild-type and mutant PLCη2 were transiently transfected into COS7 cells by electroporation and [^{3}H]inositol phosphate release was assayed as described previously (Popovics *et al.*, 2011). Briefly, transfected cells were seeded onto 12-well plates. After 24 h, cells were labelled overnight with 1 μCi/ml myo-D-[^{3}H]inositol (Perkin-Elmer, Cambridge, UK) in inositol-free DMEM (MP Biomedicals, Illkirch, France) in the absence of serum. Cells were stimulated with 0-70 μM monensin (Sigma-Aldrich, Poole, UK) at 37ºC for 3 h following addition of fresh HEPES-buffered DMEM containing 10 mM LiCl to enable accumulation of inositol phosphates. Stimulation was terminated by the removal of the medium and addition of 10 mM formic acid. The ^{3}H-labelled inositol phosphates were isolated from the extracts using Dowex AG 1-X8 ion exchange resin (BioRad), eluted with 1 M ammonium formate/0.1 M formic acid and quantified by liquid scintillation counting.

For experiments investigating Ca^{2+}-sensitivity, transfected cells were seeded into 15 cm diameter dishes and the phosphatidylinositol pool was labeled with 1 μCi/ml myo-D-[^{3}H]inositol in inositol-free DMEM containing 10% fetal calf serum. Cells were trypsinized and resuspended in permeabilization buffer (20 mM PIPES, 129 mM potassium glutamate, 5 mM glucose, 5 mM ATP, 5.31 mM $MgCl_2$, 5 mM EGTA, 10 mM LiCl, 0.1% BSA, pH 6.6). Cells were counted and electrically permeabilized (10 discharges of 3 kV/cm^3) using a custom-made device. Varying quantities of $CaCl_2$ were added to give appropriate free calcium concentrations when in equilibrium with 5 mM EGTA at pH 6.6 (Portzehl *et al.*, 1964). The cell suspensions were incubated at 37ºC for 2 h before addition of formic acid (10 mM final concentration). ^{3}H-labelled inositol phosphates were isolated and measured as described above. Results were normalized to counts/number of cells and expressed as fold changes relative to basal levels. All [^{3}H]inositol phosphate release assays were performed in triplicate and the results presented are representative of multiple experiments.

Immunoblotting

Transfected COS7 cells were seeded onto 6-well plates. Cells were scraped 48 h post-transfection in RIPA buffer containing complete protease inhibitor cocktail (Roche, Burgess Hill, UK). Cell lysates were resuspended in equal volumes of gel running buffer (125 mM Tris-HCl, 20% glycerol, 4% SDS and 90 mM β-mercaptoethanol, pH 6.8). Samples were separated by NuPAGE gradient (4-12% Bis-Tris) gel electrophoresis using a MES buffer system (Invitrogen) then electro-blotted for 75 min at 30 mA/gel onto PVDF membrane (GE Healthcare, Hertfordshire, UK). Blots were incubated for 1 h at room temperature in blocking buffer (5% non-fat milk in TBS) before being incubated for 90 min in 1% non-fat milk and 0.5% Tween-20 in TBS containing either goat polyclonal anti-PLCη2 antibody (Santa Cruz Biotechnology, Heidelberg, Germany) or mouse monoclonal anti-β-actin antibody (Sigma-

Aldrich). Blots were washed 3 times in TBST (TBS containing 0.5% Tween) after antibody incubations. Specific antibody binding was detected by chemiluminescence with horseradish peroxidase–conjugated secondary antibody and chemiluminescent substrate (both Thermo Fisher Scientific, Loughborough, UK) using a LAS-3000 imager (Fujifilm, Düsseldorf, Germany).

Molecular modeling

A molecular model of the EF-hand domain of PLCη2 was constructed based upon the structure of calmodulin (CaM) (PDB: 3EVU; Wang *et al.*, 2008) using the Modeller 9v1 program (Marti-Renom *et al.*, 2000). Despite the relatively low sequence identity between PLCη2 and CaM (~30%), the alignment between template and target sequence is unambiguous for EF-loop 1 (see Figure 1D, *Hs*CaMEF1 and *Mm*PLCη2). Due to the one residue insertion into PLCη2 within the EF-loop 2, either of His296 and Gln297 can in principle be aligned to position 'Z' depending on the positioning of the gap. To account for these two possibilities and to avoid bias, all alignment-based constraints for His296 and Gln297 were omitted during the modeling process. The resulting models were inspected manually to identify which of the two residues is a more likely candidate to ligate Ca^{2+}.

Results

Analysis of EF-hand domains from PLCη enzymes

Analysis of conserved domains from PLCη enzymes suggest that in addition to an EF-hand-like domain, which is found in most vertebrate PLC enzymes (and generally has little or no affinity toward Ca^{2+}), the η-class of phospholipase C enzymes may possess an additional functional EF-hand domain containing a pair of Ca^{2+}-binding EF-loops (Figure 1A). EF-loops are defined here as the structural motifs present within the EF-hand domain responsible for

Ca^{2+}-binding. Paired EF-loops are usually only found in Ca^{2+}-effector proteins (Gifford *et al.*, 2007). Indeed, the sequences corresponding to these domains in both PLCη proteins are conserved relative to the EF-hands of other proteins. Canonical EF-loops consist of 12 residues and have the consensus sequence DXB(G/X)(B/S)GXΨXXX(E/D), where B indicates either Asn/Asp and Ψ indicates a hydrophobic residue (Gifford *et al.*, 2007). These loops provide 7 O-ligands (named "X", "Y", "Z", "-X", "-Y", "$-Z_1$" and "$–Z_2$") to form a septadentate Ca^{2+} site as illustrated in Figures 1B and 1C. However, the second of the two putative EF-loops in PLCη enzymes appears to contain 13 residues, representing a novel type of non-canonical EF-loop (Figure 1D). The sequence alignment reveals that the "extra residue" in EF-loop 2 is most likely to be either H296 or Q297 at positions 5 and 6, respectively. This 13-residue loop is conserved in all known vertebrate PLCη enzymes (including mammals, amphibians, birds and fish; Figure S1), suggesting that this motif is (or was) functionally important and originated (probably due to a codon insertion event) prior to the divergence of vertebrates 500 million years ago. Non-canonical loops have been identified in a number of EF-hand-containing proteins, which in some cases are able to co-ordinate to Ca^{2+} (Gifford *et al.*, 2007; Grabarek, 2006). An example (human calbindin D_{9K}) is illustrated in the alignment in Figure 1D. The first of the two EF-loops in this protein contains an additional Ala residue between what would correspond to the canonical 1st and 2nd residues and a Pro residue between the 5th and 6th. Structural studies reveal that in this case the co-ordinating ligands "X", "Y" and "Z" are provided by the backbone carbonyl groups rather than the amino acid side-chains (Kördel *et al.*, 1993).

Ca^{2+}-binding properties of synthetic PLCη2 EF-loop peptides

In order to probe whether and how Ca^{2+} may co-ordinate to the EF-loops within the EF-hand domain of PLCη2, we generated synthetic peptides corresponding to each of the two putative

Ca^{2+}-binding loops and as a control, the first EF-loop of CaM. NMR spectra (2D ^{1}H TOCSY and NOESY) were recorded for each of the three peptides in the presence and absence of 5 mM Ca^{2+} (2D ^{1}H TOCSY spectra are shown in Figure 2). The addition of a 5-fold molar excess of Ca^{2+} to the peptides elicited significant changes in chemical shifts of the backbone NH protons of both PLCη2 EF-loop peptides, comparable to those observed for the CaM EF-loop 1 peptide (as summarized in Figure 3). A titration with up to 500 mM Ca^{2+} for loop 2 gave a dissociation constant of K_D = 20 ± 4 mM in aqueous solution (Figure S2). Since the overall magnitude of the observed effects at 5 mM Ca^{2+} were similar for all three peptides, it is clear that Ca^{2+} binding to all three isolated loops was, as expected, considerably weaker than to intact EF-hand motifs (Borin *et al.*, 1989). It can be estimated that at the concentrations used for the 2D ^{1}H NMR experiments (1 mM peptide, 5 mM Ca^{2+}), a mixture of bound and unbound peptides was present. Only a single set of resonances was observed in either the presence or absence of Ca^{2+} for all peptides, indicating that the systems are in fast exchange on the NMR timescale. Hence, the resonances observed in the presence of Ca^{2+} also correspond to a mixture between peptides with and without Ca^{2+} bound, with the magnitude of the chemical shift perturbation reporting qualitatively on the overall effect of Ca^{2+} binding on each individual residue. The residues experiencing the largest shift perturbation were those in positions 3 (“X”), 5 (“Y”), and 8 (residue after “Z”) in all three peptides. One of the side-chain amide protons of N5 (“Y”; PLCη2 loop 1) also experienced a clear change in shift (0.026 ppm), supporting the involvement of the adjacent carbonyl oxygen in Ca^{2+}-binding. The similarity of the chemical shift perturbation patterns also suggested that in the EF-loop 2 peptide, H7 corresponds to residue “Z”, and indeed, its side-chain protons were significantly affected by the presence of Ca^{2+} (Hε1: $\Delta\delta$ = 0.037 ppm; also see Figure S2 for titration data in aqueous solution), suggesting an involvement in Ca^{2+}-binding. The side-chain amide protons of Q8 experienced changes in chemical shift (<0.02 ppm in DMSO-d_6 in the presence

and absence of Ca^{2+}; titration data could not be fitted satisfactorily). Furthermore, T12 (residue after "-X") in the CaM EF-loop 1 peptide also shifted considerably; this behavior was not observed for either of the two PLCη2 loops. In addition, the NH resonance for K13 (CaM EF-loop 1) was not observed in either presence or absence of Ca^{2+}, whereas the corresponding residues were readily identified in the two PLCη2 loop peptides. These subtle differences may hint at structural variations in the C-terminal portions of the loops. It is also noteworthy that residue "-X" usually binds through a water molecule interacting with the side-chain of this residue; whilst the serine residue in loop 1 permits this, such an interaction is not possible with the glycine "-X" residue in PLCη2 EF-loop 2. In summary, both loops appear to have, *in vitro*, the ability to bind Ca^{2+} in a manner that is similar to that of canonical EF-loops for the N-terminal portion, with likely variations in the C-terminal half.

EF-loop 1 is important for PLCη2 activity

The role of the EF-hand domain in activation of PLCη2 was investigated by site-directed mutagenesis. This was achieved by measuring the accumulation of released inositol phosphate in intact COS7 cells expressing wild-type PLCη2, and five EF-hand domain mutants (D256A from EF-loop 1 and D292A, H296A, Q297A and E304A from EF-loop 2) following treatment with monensin. Monensin is a Na^+/H^+ antiporter (which acts to increase cytosolic Na^+ levels) was previously found to be extremely effective in activating exogenous PLCη2 in these cells. This is initiated largely by an increase in cytosolic Ca^{2+} via the mitochondrial Na^+/Ca^{2+}-exchanger as this activity has been shown to be greatly inhibited by the specific inhibitor, CPG37157 (Popovics *et al.*, 2011).

COS7 cells transiently expressing the wild-type enzyme exhibited a concentration-dependent increase in inositol phosphate accumulation (indicative of PLC activity) in response to

monensin treatment relative to empty vector control (Figures 4A and 4B). Inositol phosphate accumulation was typically increased by ~4 to 7-fold at the highest concentration used (70 μM). This varied a bit between assays due to differences in transfection efficiency. A small increase in PLC activity was observed in control cells but was <2-fold higher than basal level following treatment with 70 μM monensin. This was likely due to a Ca^{2+}-induced increase in basal PLC activity. Although PLCη2 is not endogenously expressed in COS7 cells (Stewart *et al.*, 2007), multiple PLCs are present in most cell types. Increased intracellular Ca^{2+} levels would likely enhance basal activity as Ca^{2+} is required for both catalysis and membrane binding. Monensin treatment did not lead to an increase in PLC activity in cells expressing the D256A mutant, suggesting that this residue is important for Ca^{2+}-dependent PLCη2 activity. In cells expressing the D292A mutant, inositol phosphate release was increased but was 20% less than the wild-type enzyme. Monensin treatment of cells expressing the H296A, Q297A or E304A mutants exhibited similar increases in inositol phosphate release as those expressing the wild-type enzyme. Immunoblotting of lysates from transfected cells with anti-PLCη2 antibody confirmed that wild-type and mutant proteins were expressed in each case.

Ca^{2+}-sensitivity of PLCη2 is conferred by EF-loop 1

To establish whether the EF-hand domain is responsible for Ca^{2+}-dependent activation of PLCη2, we examined inositol phosphate accumulation in permeabilized COS7 cells expressing the wild-type and mutant enzymes at a range of free calcium concentrations (Figure 5). Wild-type PLCη2 activity was extremely sensitive to Ca^{2+}, exhibiting a sharp increase in activity at concentrations between 0.1 and 1 μM free Ca^{2+} as previously reported (Popovics *et al.*, 2011). Endogenous PLCs (as indicated in control cells) also exhibited a Ca^{2+}-dependent increase in activity but were less sensitive with the highest increase observed between 1 and 10 μM free Ca^{2+}. Significantly, 1 μM free Ca^{2+} was not sufficient to stimulate

activity of the D256A enzyme. However, activity was observed in the presence of 10 μM free Ca^{2+} relative to control cells, consistent with a ~10-fold drop in Ca^{2+}-sensitivity relative to the wild-type enzyme. The activity of the D292A, H296A, Q297A and E304A enzymes in the presence of 1 μM free Ca^{2+} were similar to the wild-type enzyme. However, the activities of H296A, Q297A and E304A mutants (but not the D292A mutant) were lower than that of the wild type at the highest concentrations of free Ca^{2+} (10 mM and 100 mM; data not shown). Although the Ca^{2+}-sensitivity of the D256A protein was 10-fold lower than the wild type enzyme this does not necessarily equate to only a 10-fold reduction in the affinity of EF-loop 1 toward Ca^{2+} (in fact the mutation may well have a much greater effect on the affinity). It is possible that there is another mechanism by which Ca^{2+} activates the enzyme when the free Ca^{2+} concentration is above 1 μM. This is in part supported by the observation that PLCδ1 exhibits a similar Ca^{2+}-sensitivity to the D256A mutant (maximal activity at 10 μM; Nakahara *et al.*, 2005) yet does not possess the additional EF-hand domain found within the PLCη enzymes.

Molecular model of the PLCη2 EF-hand domain

In the absence of structural data for PLCη2, a 3D-model of the murine PLCη2 EF-hand domain, consisting of two conjugated helix-loop-helix motifs, was built using the crystal structure co-ordinates of CaM (PDB: 3EVU; Wang *et al.*, 2008). In the model, two 7-co-ordinate Ca^{2+} atoms are bound to each EF-loop with pentagonal bipyramidal geometries (Figure 6). In the first EF-loop the metal binding site is composed of five residues; Asp256, Asn258, Asp260, Ser262 (backbone oxygen) and Glu267 (two ligands). A 7^{th} O-ligand is provided by a water molecule held in position by an H-bond to the side-chain of Ser264. For the second EF-loop 2, the residues Asp292, Asp294, Thr299 (backbone oxygen) and Glu304 provide 5 ligands, with two coming from Glu304. In this model His296 is in a position where

it seems feasible that it may also contribute to Ca^{2+} binding, in agreement with the NMR-data for the EF-loop 2 construct, but alternative models in which Gln297 provides a sidechain amide oxygen are also plausible. An additional water molecule was modeled to complete the co-ordination sphere.

Discussion

Analysis of PLCη sequences has revealed that this PLC class contains a novel EF-hand domain that includes a non-canonical EF-loop 2 sequence. This unusual EF-loop consists of 13 residues (rather than 12). A 13 residue EF-loop is also found within osteonectin (also called BM-40), an extracellular matrix protein where it is the first EF-loop of the pair that contains an amino acid insertion between the residues at positions 3 and 4 (Hohenester *et al.*, 1996). Sequence alignment of EF-hands with those from other proteins suggested the extra residue in PLCη2 may either have been H296 at position 5 or Q297 at position 6 of the loop.

An attempt to generate a recombinant fragment of PLCη2 containing the EF-hand domain for further study was unsuccessful as the resultant protein was found to be unstable (data not shown). Short EF-loop peptides have previously been used as models to probe the structural and metal-binding properties of such regions (Marsden *et al.*, 1989; Prod'hom and Karplus, 1993). Thereby in order to determine whether the EF-loops are able to co-ordinate Ca^{2+}, and more specifically which EF-loop residues may co-ordinate Ca^{2+}, 2D ^{1}H TOCSY and NOESY NMR spectra were recorded for synthetic peptides corresponding to EF-loops 1 and 2 of PLCη2 and EF-loop 1 of CaM (as a control) in the presence and absence of 5 mM Ca^{2+}. The prevailing constitutional and conformational equilibria render a structure determination from the peptide NMR data impractical, but analysis of chemical shift perturbation of amide protons upon Ca^{2+}-binding gave qualitative hints on residues likely involved in Ca^{2+} co-

ordination. The differences in amide proton shifts suggested that the N-terminal portions of both PLCη2 EF-loop peptides are likely to co-ordinate the metal in a similar manner to that of the canonical CaM EF-loop 1, but greater differences were seen in the C-terminal portions of the loops. Of key importance was to attempt to determine whether the side-chain from either H296 or Q297 could provide the "Z" ligand within the second EF-loop of PLCη2. Interestingly, Q297 is fully conserved among vertebrate PLCη2 sequences (Figure S1). Glutamine side-chains commonly provide Ca^{2+}-ligands in proteins (Harding, 2004). However, the involvement of protein histidine side-chains in Ca^{2+}-binding has also been reported (Yoshioka *et al.*, 1997; Eichinger *et al.*, 1999; Bouckaert *et al.*, 2000), although this particular interaction is quite rare (Harding, 2004). A large shift difference recorded for the side-chain protons of H7 in the PLCη2 EF-loop 2 peptide, characterized by a defined dependence on Ca^{2+} concentration that can be fitted with a single dissociation constant, suggested that this residue (which corresponds to H296 in the full length protein) is a strong candidate for providing the "Z" ligand for Ca^{2+}-binding in this loop. Hence, both isolated PLCη2 EF-loops were capable of interacting with Ca^{2+} *in vitro*. A molecular model of the EF-hand domain was constructed based upon the structure of CaM with Ca^{2+} ions bound at each of the two EF-loops. Only minor rearrangements were required to accommodate the metal in each case, suggesting that both sites could potentially participate in Ca^{2+}-binding in the PLCη2 protein. The model supported the involvement of H296 contributing to Ca^{2+}-binding in EF-loop 2, as suggested by the peptide experiments.

Supported by the information gleaned from the NMR studies, the role of the EF-hand domain in Ca^{2+}-induced PLCη2 activation was investigated by site-directed mutagenesis in live cells. The D256 residue within EF-loop 1 was mutated to alanine. This particular residue was chosen to be substituted as it is conserved within EF-loops from other proteins and is known

to provide the "X" ligand. Involvement of this residue in binding Ca^{2+} is also supported by the peptide NMR data; the amide protons of the corresponding residue in the EF-loop 1 peptide undergo a characteristic chemical shift change upon addition of Ca^{2+}. Four residues were mutated to alanine within EF-loop 2. These included D292 and E304 which were chosen because residues at these positions are known to provide Ca^{2+}-binding "X" and "-Z" ligands, respectively in (canonical) EF-loops of other proteins (Gifford *et al.*, 2007). The H296 and Q297 residues were also mutated as likely candidates to constitute the "extra residue" uniquely found within PLCη2 EF-loop 2 sequences, and either could correspond to the "Z" residue.

As previously reported, cells expressing wild-type PLCη2 exhibited a concentration-dependent increase in inositol phosphate accumulation in response to monensin treatment (Popovics *et al.*, 2011). The D256A mutation had a dramatic effect upon the ability of the enzyme to respond to monensin-induced elevations in $[Ca^{2+}]_i$. In contrast, increases in inositol phosphate accumulation were observed in cells expressing the D292A, H296A, Q297A and E304A mutants that were similar to those observed in cells expressing the wild-type enzyme. It should be noted that this effect was slightly reduced (*ca.* 20%) in D292A. If Ca^{2+}-binding to EF-loop 2 was important for PLCη2 activity then it would be expected that at least one of the four mutations would influence Ca^{2+}-binding and greatly perturb the ability of the enzyme to respond to monensin-induced Ca^{2+} influx. These results suggest that Ca^{2+}-binding to EF-loop 1, but not EF-loop 2 is important for PLCη2 activity.

To determine whether the EF-hand domain is directly involved in sensing Ca^{2+}, inositol phosphate accumulation was examined in permeabilized COS7 cells transiently expressing the wild-type and mutant proteins at a range of free Ca^{2+} concentrations. The wild-type

enzyme exhibited the greatest increase in activity at free Ca^{2+} concentrations between 0.1 μM and 1 μM relative to the control cells. This finding is in agreement both with our previous observations (Popovics *et al.*, 2011), and studies by Nakahara *et al.* (2005) who have measured the activity of recombinant PLCη2 in the presence of Ca^{2+}. As expected the D256A mutant was unable to respond to 1 μM free Ca^{2+} but was active in the presence of 10 μM free Ca^{2+}. This corresponds to a ~10-fold reduction in Ca^{2+} sensitivity. Basal PLC activity due to endogenously expressed PLC enzymes was also optimal at 10 μM free Ca^{2+} and was similar to that previously observed for PLCδ1 (Nakahara *et al.*, 2005). Hence when Ca^{2+}-binding to EF-loop 1 is disrupted, PLCη2 exhibits a Ca^{2+}-dependence similar to that of PLCδ1. The EF-loop 2 mutations had no effect upon Ca^{2+}-sensitivity, as with the wild-type enzyme, these mutants exhibited maximal activity in the presence of 1 μM free Ca^{2+} (data not shown). Interestingly, the activity of the D292A mutant at 1 μM of free Ca^{2+} was ~20% less than wild-type PLCη2 (as observed in the intact cell assay); this may be due to a difference in protein expression or the mutation may cause a conformational change that alters the ability of the EF-hand to "communicate" with the catalytic domains. The permeabilized cell experiments largely reflected the results observed in the intact cells treated with monensin given that this agent is likely to increase $[Ca^{2+}]_i$ to ~1 μM.

Collectively, these results suggest that EF-loop 1 of PLCη2 is able to bind submicromolar concentrations of free Ca^{2+}, which in turn alter the conformation of the enzyme such that its ability to hydrolyze PIP_2 is enhanced. The EF-loop 2 mutations had no great effect upon activity suggesting this loop may either not bind Ca^{2+} at physiological concentrations, or that Ca^{2+}-binding does not affect PLCη2 activity. Although the synthetic EF-loop 2 peptide was shown to bind to Ca^{2+} in a similar manner to either EF-loop1 or a CaM control peptide (albeit at higher than physiological concentration), this loop may exhibit similar behavior when part

of the full length protein. An EF-hand domain with a non-functional second EF-loop is not without precedent; the sarcoplasmic Ca^{2+}-binding protein (SCP) from the sandworm, *Nereis diversicolor* possesses an EF-hand domain with a non-functional second loop (Vijay-Kumar and Cook, 1992). Although this protein is thought to function as a Ca^{2+} buffer rather than an effector protein, NMR and circular dichroic studies of apo- and metal bound-SCP reveal that the binding of 1 mole equivalent of Ca^{2+} invokes a significant change in the conformation of the protein; SCP has a highly unstructured apo state which is switched to the native state upon binding of the first Ca^{2+} ion (Prêcheur *et al.*, 1996). It is therefore conceivable that Ca^{2+}-binding at the first EF-loop of PLCη2 alone is sufficient to allosterically control catalysis. The function of the EF-hand-like domain (residues 317-399) in PLCη2 is unknown but it is possible that it plays a role in translating Ca^{2+}-binding by the EF-hand domain discussed here to the catalytic domain.

In conclusion, we provide the first evidence that the EF-hand domain of PLCη2 is responsible for activation by Ca^{2+} and highlight the involvement of EF-loop 1 in mediating this effect. Further work is required to establish whether both EF-loops bind Ca^{2+} under physiological conditions, to resolve whether EF-loop 2 binds Ca^{2+} too weakly, or with in principle sufficient strength, but without influencing enzyme activity.

Acknowledgement

We gratefully acknowledge the University of St Andrews (PhD studentship to Petra Popovics), The Royal Society (Olga Kennard Fellowship to Claudia A. Blindauer), and the EPSRC and BP (Dorothy Hodgkin Fellowship to Jin Lu).

References

Bairoch A, Cox JA. 1990. EF-hand motifs in inositol phospholipid-specific phospholipase C. FEBS Lett 269:454-456.

Bax A, Davis DG. 1985. MLEV-17-Based Two-Dimensional Homonuclear Magnetization Transfer Spectroscopy. J Magn Reson 65:355-360.

Berridge MJ, Lipp P, Bootman MD. 2000. The versatility and universality of calcium signalling. Nat Rev Mol Cell Biol 1:1-21.

Borin G, Ruzza P, Rossi M, Calderan A, Marchiori F, Peggion E. 1989. Conformation and ion binding properties of peptides related to calcium binding domain III of bovine brain calmodulin. Biopolymers 28:353-369.

Bouckaert J, Dewallef Y, Poortmans F, Wyns L, Loris R. 2000. The structural features of concanavalin A governing non-proline peptide isomerisation. J Biol Chem 275:19778-19787.

Burgoyne RD. 2004. The neuronal calcium sensor proteins. Biochim Biophys Acta 1742:59-68.

Drabikowski W, Brzeska H, Venyaminov SY. 1982. Tryptic fragments of calmodulin. Ca^{2+}- and Mg^{2+}-induced conformational changes. J Biol Chem 257:11584-11590.

Eichinger A, Beisel HG, Jacob U, Huber R, Medrano FJ, Banbula A, Potempa J, Travis J, Bode W. 1999. Crystal structure of gingipain R: an Arg-specific bacterial cysteine proteinase with a caspase-like fold. EMBO J 18:5453-5462.

Gaggelli E, D'Amelio N, Maccotta A, Valensin G. 1999 Calcium-binding properties and molecular organization of bradykinin - A solution H-1-NMR study. Eur J Biochem 262:268-276.

Gifford JL, Walsh MP, Vogel HJ. 2007. Structures and metal-ion-binding properties of the Ca^{2+}-binding helix-loop-helix EF-hand motifs. Biochem J 405:199-221.

Grabarek Z. 2006. Structural basis for diversity of the EF-hand calcium-binding proteins. J Mol Biol 359:509-525.

Harding MM. 2004. The architecture of metal coordination groups in proteins. Acta Crystallogr D Biol Crystallogr D60:849-859.

Hohenester E, Maurer P, Hohendahl C, Timpl R, Jansonius JN, Engel J. 1996. Structure of a novel extracellular Ca^{2+}-binding module in BM-40. Nat Struct Biol 3:67-73.

Hwang JI, Oh YS, Shin KJ, Kim H, Ryu SH, Suh PG. 2005. Molecular cloning and characterization of a novel phospholipase C, PLC-η. Biochem J 389:181-186.

Hwang TL, Shaka AJ. 1995. Water suppression that works. Excitation sculpting using arbitrary waveforms and pulsed field gradients. J Magn Reson A 112:275-279.

Kim JK, Choi JW, Lim S, Kwon O, Seo JK, Ryu SH, Suh PG. 2011. Phospholipase C-η1 is activated by intracellular Ca^{2+} mobilization and enhances GPCRs/PLC/Ca^{2+} signaling. Cell Signal 23:1022-1029.

Kördel J, Skelton NJ, Akke M, Chazin WJ. 1993. High-resolution structure of calcium-loaded calbindin D9k. J Mol Biol 231:711-734.

Kouchi Z, Shikano T, Nakamura Y, Shirakawa H, Fukami K, Miyazaki S. 2005. The role of the EF-hand domains and C2 domain in regulation of enzymatic activity of phospholipase Cζ. J Biol Chem 280:21015-21021.

Marcus Y. 1984. The effectivity of solvents as electron pair donors. J Solut Chem 13:599-624.

Marion D, Ikura M, Tschudin R, Bax A. 1989. Rapid recording of 2D NMR spectra without phase cycling. Application to the study of hydrogen exchange in proteins. J Magn Reson 85:393-399.

Marsden BJ, Hodges RS, Sykes BD. 1989. A ^{1}H NMR determination of the solution conformation of a synthetic analogue of calcium-binding site III of rabbit skeletal troponin C. Biochemistry 28:8839-8847.

Marti-Renom MA, Stuart A, Fiser A, Sánchez R, Melo F, Sali A. 2000. Comparative protein structure modeling of genes and genomes. Annu Rev Biophys Biomol Struct 29:291-325.

Nakahara M, Shimozawa M, Nakamura Y, Irino Y, Morita M, Kudo Y, Fukami K. 2005. A novel phospholipase C, PLCη2, is a neuron-specific isozyme. J Biol Chem 280:29128-29134.

Oliva R, Falcigno L, D'Auria G, Saviano M, Paolillo L, Ansanelli G, Zanotti, G. 2000. Bicyclic peptides as models of calcium binding sites: Synthesis and conformation of a homodetic undecapeptide. Biopolymers 5:581-595.

Parmacek MS, Leiden JM. 1991. Structure, function, and regulation of troponin C. Circulation 84:991-1003.

Popovics P, Beswick W, Guild SB, Cramb G, Morgan K, Millar RP, Stewart AJ. 2011. Phospholipase C-η2 is activated by elevated intracellular Ca^{2+} levels. Cell Signal 23:1777-1784.

Popovics P, Gray A, Arastoo M, Finelli DK, Tan AJL, Stewart AJ. 2013. Phospholipase C-η2 is required for retinoic acid-stimulated neurite growth. J Neurochem 124:632-644.

Portzehl H, Caldwell PC, Rüegg JC. 1964. The dependence of contraction and relaxation of muscle fibres from the crab *Maia squinado* on the internal concentration of free calcium ions. Biochim Biophys Acta 79:581-591.

Prêcheur B, Cox JA, Petrova T, Mispelter J, Craescu CT. 1996. *Nereis* sarcoplasmic Ca^{2+}-binding protein has a highly unstructured apo state which is switched to the native state upon binding of the first Ca^{2+} ion. FEBS Lett 395:89-84.

Prod'hom B, Karplus M. 1993. The nature of the ion binding interactions in EF-hand peptide analogs: free energy simulation of Asp to Asn mutations. Protein Eng 6:585-592.

Stewart AJ, Morgan K, Farquharson C, Millar RP. 2007. Phospholipase C-eta enzymes as putative protein kinase C and Ca^{2+} signalling components in neuronal and neuroendocrine tissues. Neuroendocrinology 86:243-248.

Stewart AJ, Mukherjee J, Roberts SJ, Lester D, Farquharson C. 2005. Identification of a novel class of mammalian phosphoinositol-specific phospholipase C enzymes. Int J Mol Med 15:117-121.

Strynadka NC, James MN. 1989. Crystal structures of the helix-loop-helix calcium-binding proteins. Annu Rev Biochem 59:951-998.

Vetter SW, Leclerc E. 2003. Novel aspects of calmodulin target recognition and activation. Eur J Biochem 270:404-414.

Vijay-Kumar S, Cook WJ. 1992. Structure of a sarcoplasmic calcium-binding protein from *Nereis diversicolor* refined at 2.0 Å resolution. J Mol Biol 224:413-426.

Wang Q, Shui B, Kotlikoff MI, Sondermann H. 2008. Structural basis for calcium sensing by GCaMP2. Structure 16:1817-1827.

Yamamoto T, Takeuchi H, Kanematsu T, Allen V, Yagisawa H, Kikkawa U, Watanabe Y, Nakasima A, Katan M, Hirata M. 1999. Involvement of EF hand motifs in the Ca^{2+}-dependent binding of the pleckstrin homology domain to phosphoinositides. Eur J Biochem 265:481-490.

Yeagle PL, Bennett M, Lemaitre V, Watts A. 2007. Transmembrane helices of membrane proteins may flex to satisfy hydrophobic mismatch. Biochim Biophys Acta 1768:530-537.

Yoshioka Y, Hasegawa K, Matsuura Y, Katsube Y, Kubota M. 1997. Crystal structures of a mutant maltotetraose-forming exo-amylase cocrystallized with maltopentose. J Mol Biol 271:619-628.

Zhou Y, Wing MR, Sondek J, Harden TK. 2005. Molecular cloning and characterization of PLC-η2. Biochem J 391:667-676.

Figure Legends

Fig. 1. (A) Domain structure of phospholipase C-η2. PH, pleckstrin homology domain; EF, EF-hand domain; EFL, EF-hand-like domain; Cat X and Cat Y, catalytic domains; C2, Ca^{2+}-dependent membrane binding domain. (B) Sequence preference of EF-loops (modified from Gifford *et al.*, 2007). Ligands "X", "Y", "Z", "-X", "-Y", "-Z_1" and "-Z_2" are indicated by their position in the loop and whether co-ordination occurs via side-chain or backbone carbonyl oxygens. Ligand "-X" is a water molecule H-bonded to the side-chain. Note that residue 12 is usually a bidentate ligand (contributing both "-Z_1" and "-Z_2" ligands), i.e. side-chain carboxylate oxygens of either Glu or Asp. In the Ca^{2+}-bound state the ligands co-ordinate forming a pentagonal bipyramid geometry around the Ca^{2+} ion as shown in (C). The "Y", "-Y", "Z", "-Z_1" and "-Z_2" ligands align along the vertices of an approximately planar pentagon with ligands "X" and "-X" in an axial position ~90° to the other five (Strynadka and James, 1989). (D) Partial sequence alignment of EF-hand domains of PLCη enzymes and other proteins. Each of the two EF-loops is indicated by the box. *Mm*PLCη2, murine phospholipase C-η2; *Hs*PLCη2, human phospholipase C-η2; *Hs*PLCη1, human phospholipase C-η1; *Hs*CaMEF1, human calmodulin EF-hand domain 1; *Hs*CaMEF2, human calmodulin EF-hand domain 2; *Hs*TropCII, human troponin C (type2); *Hs*NCS-1, human neuronal calcium sensor-1; *Hs*CalcinB, human calcineurin B; *Hs*CalD9K, human calbindin D_{9K}.

Fig. 2. Overlays of the fingerprint region of 2D-^{1}H TOCSY NMR spectra of EF hand loop peptides in the presence (red) and absence (blue) of a 5-fold excess of Ca^{2+} (1 mM peptide, DMSO-d_6, 298 K, 500 MHz). Each set of vertically aligned peaks corresponds to a particular residue, with the chemical shift of the NH backbone protons along the x-axis (ω2); for maximal clarity, residues are labeled near their NH-side-chain cross-peaks. Changes in

chemical shifts upon calcium addition can be clearly observed for several NH protons. Residues are labeled according to their position in the peptide.

Fig. 3. Overview of the influence of Ca^{2+} (5 mM) on backbone amide resonances of EF- loop peptides corresponding to CaM EF-loop1, PLCη2 EF-loop1 and PLCη2 EF-loop 2. Residues are labeled according to their position in the peptide; for example, D3 (PLCη2 loop1) corresponds to D256 in the full length protein. The first loop of calmodulin is shown as a positive control with residues directly involved in Ca^{2+}-binding in positions 3 ("X"), 5 ("Y"), 7 ("Z"), 9("-Y"; backbone), 11 ("-X"), and 14("$-Z_1$" and "$-Z_2$"). Errors are $<\pm 0.007$ ppm.

Fig. 4. Measurement of [^{3}H]-labeled inositol phosphate accumulation in COS7 cells transfected with constructs encoding wild-type PLCη2 (and empty vector control) together with (A) D256A and D292A mutants and (B) H296A, Q297A and E304A mutants in response to monensin, respectively. Results are representative of at least three experiments and expressed ± S.E.M. Western blots confirm expression of wild-type and mutant proteins in the transfected cells.

Fig. 5. Measurement of [^{3}H]-labeled inositol phosphate accumulation in permeabilized COS7 cells transfected with constructs encoding wild-type PLCη2 (and empty vector control) together with D256A and D292A mutants in the presence of different concentrations of free Ca^{2+}, respectively. Experiments were performed simultaneously. In all cases the experiments were carried out in triplicate, the results are representative of at least three experiments and are expressed ± S.E.M.

Fig. 6. Molecular model of the EF-hand domain of mouse PLCη2 with Ca^{2+}-bound. The model was constructed using the calmodulin structure, PDB:3EVU (Wang *et al.*, 2008) as a template. Residues within the two EF-loops implicated in Ca^{2+}-binding are indicated. The question mark indicates the uncertainty as to whether EF-loop 2 participates in Ca^{2+} binding *in vivo*.

A

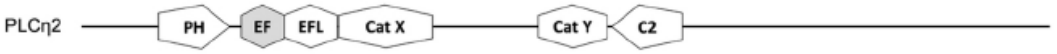

B

EF-Loop position	1	2	3	4	5	6	7	8	9	10	11	12
coordinating ligand	X side-chain		Y side-chain		Z side-chain		-Y back-bone		-X side-chain H-bond to H_2O			-Z side-chain
consensus	Asp	X	Asx	Gly/X	Asx/Ser	Gly	X	ψ	X	X	X	Glu/Asp

C

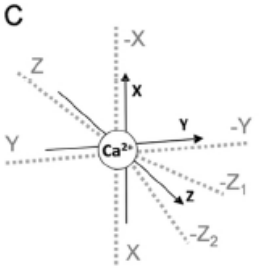

D

Figure 1

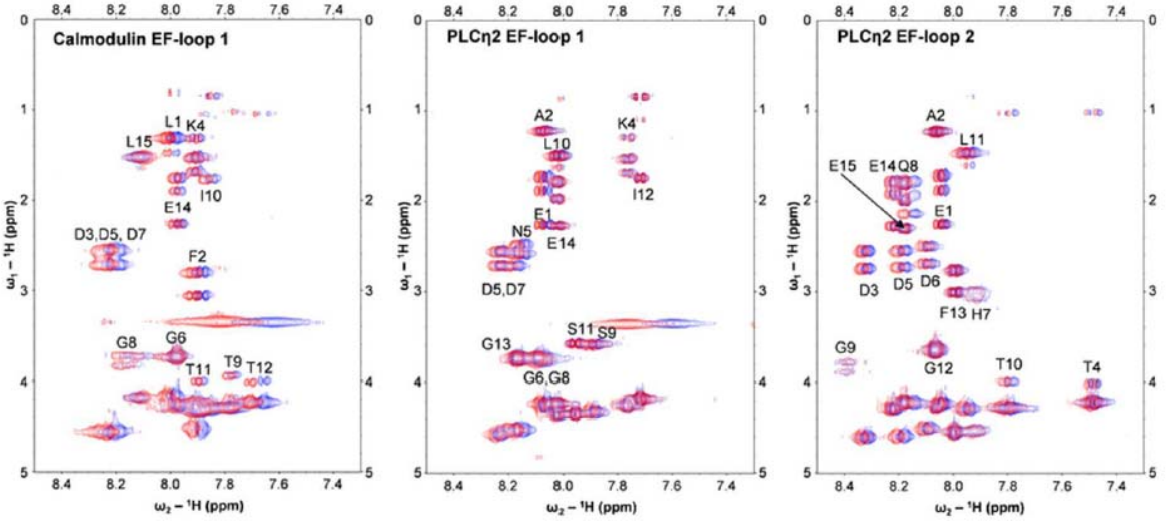
Calmodulin EF-loop 1
L1
K4
L15
I10
E14
D3,D5, D7
F2
G8
G6
T11
T9
T12
PLCη2 EF-loop 1
A2
K4
L10
I12
E1
N5
E14
D5,D7
S11
S9
G13
G6,G8
PLCη2 EF-loop 2
A2
L11
E15
E14
Q8
E1
D3
D5
D6
F13
H7
G9
G12
T10
T4
ω1 – 1H (ppm)
ω2 – 1H (ppm)

Figure 2

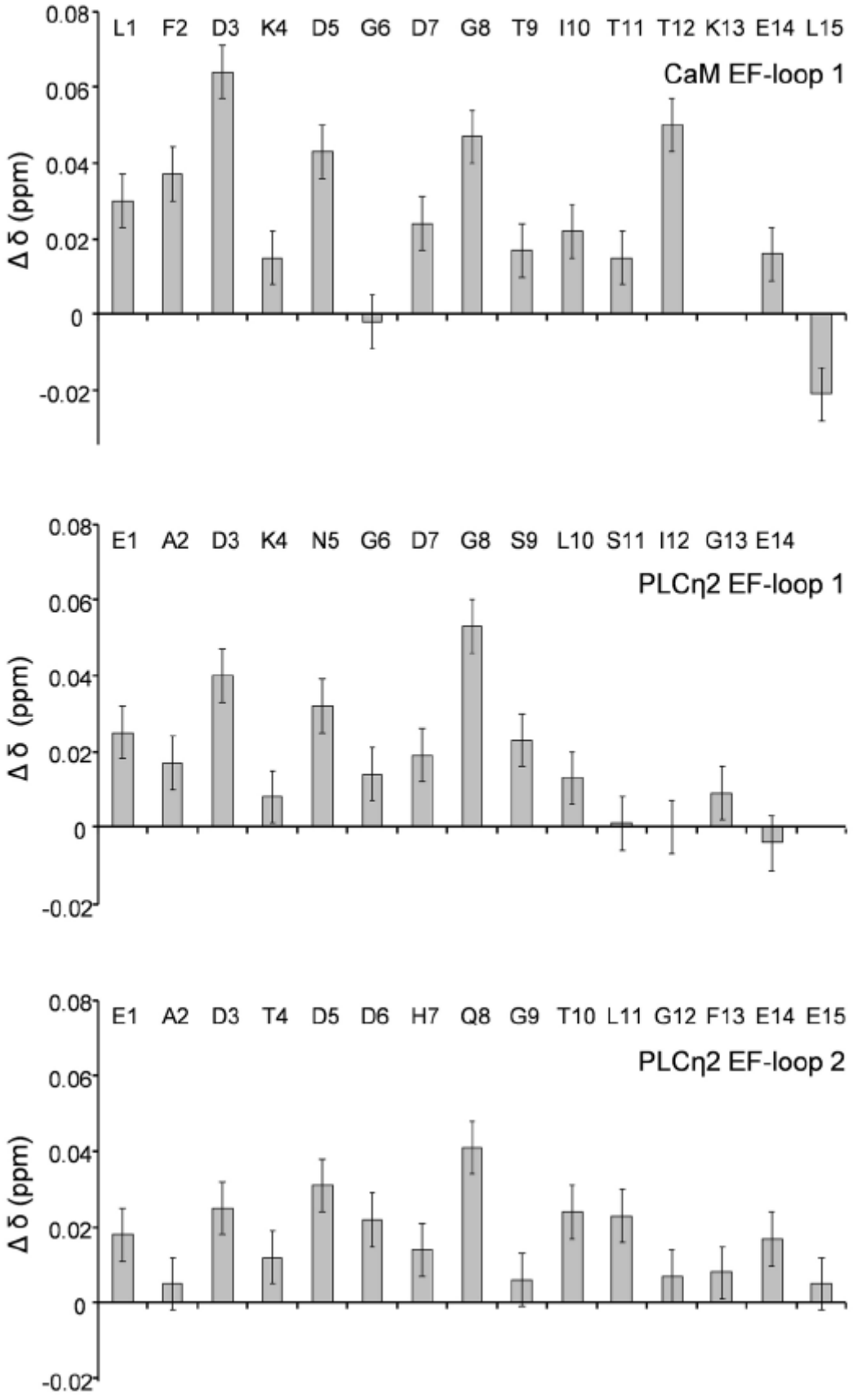
0.08
0.06
0.04
0.02
0
-0.02
Δ δ (ppm)
L1 F2 D3 K4 D5 G6 D7 G8 T9 I10 T11 T12 K13 E14 L15
CaM EF-loop 1
E1 A2 D3 K4 N5 G6 D7 G8 S9 L10 S11 I12 G13 E14
PLCη2 EF-loop 1
E1 A2 D3 T4 D5 D6 H7 Q8 G9 T10 L11 G12 F13 E14 E15
PLCη2 EF-loop 2

Figure 3

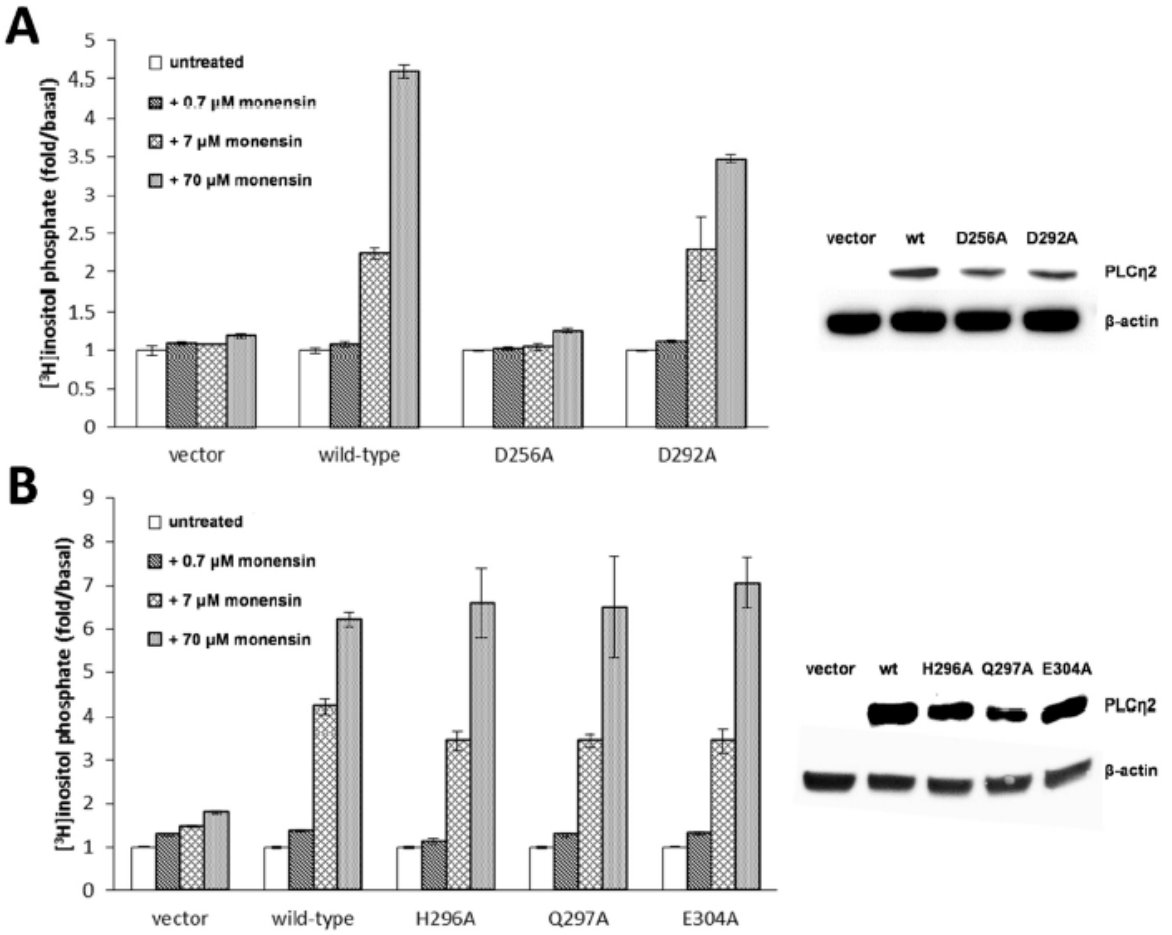
A
[3H]inositol phosphate (fold/basal)
untreated
+ 0.7 μM monensin
+ 7 μM monensin
+ 70 μM monensin
vector
wild-type
D256A
D292A
vector wt D256A D292A
PLCη2
β-actin
B
[3H]inositol phosphate (fold/basal)
untreated
+ 0.7 μM monensin
+ 7 μM monensin
+ 70 μM monensin
vector
wild-type
H296A
Q297A
E304A
vector wt H296A Q297A E304A
PLCη2
β-actin

Figure 4

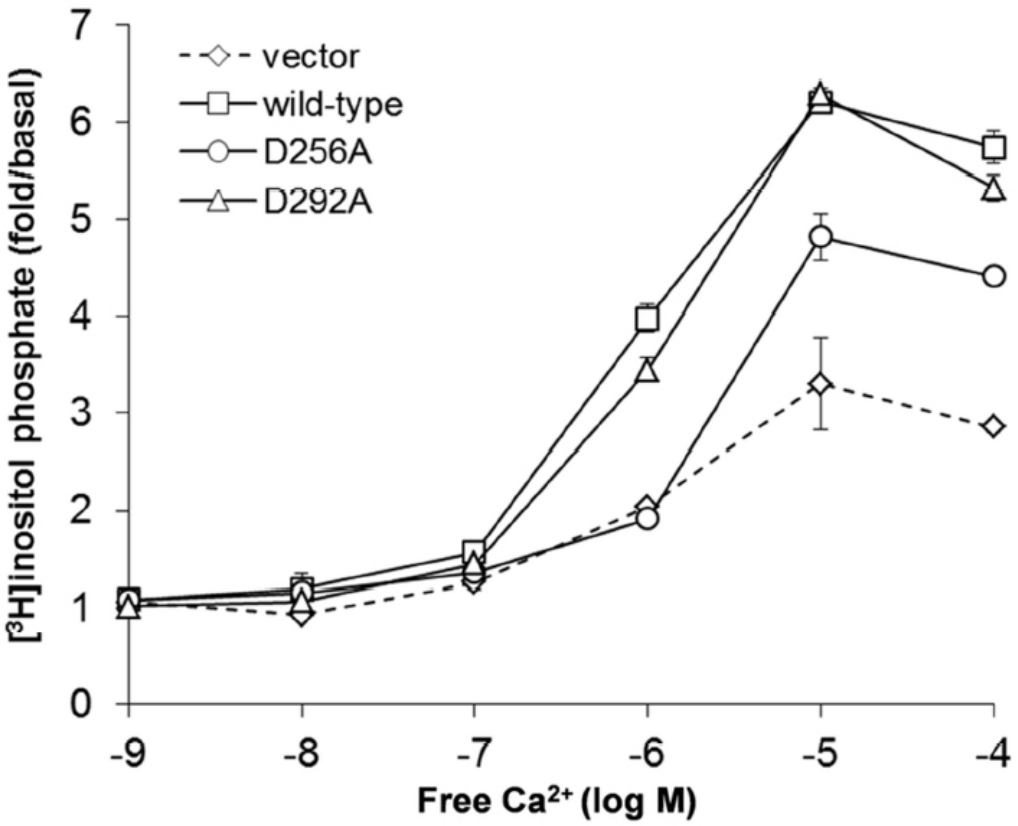
vector
wild-type
D256A
D292A
[³H]inositol phosphate (fold/basal)
Free Ca²⁺ (log M)
0
1
2
3
4
5
6
7
-9
-8
-7
-6
-5
-4

Figure 5

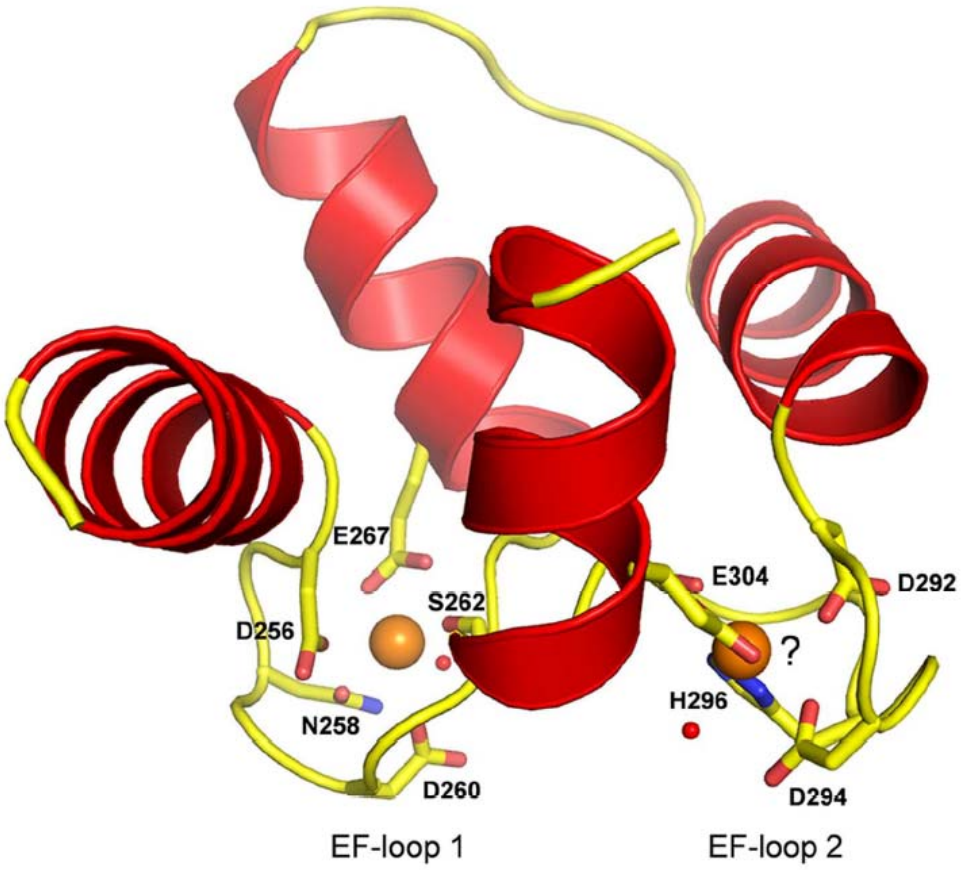
E267
S262
D256
N258
D260
E304
D292
?
H296
D294
EF-loop 1
EF-loop 2

Figure 6